An Improved Selective Harmonics Elimination Technique for PV Assisted Single Phase Grid-Tied PWM Inverter

***Abstract*-- This paper presents an improved selective harmonics elimination technique for PV assisted single phase grid-tied pulse width modulated (PWM) voltage source inverter (VSI). The switching angles are determined offline through numerical techniques and stored in microcontroller memory as a function of modulation index m_d for online application. For multiple solution, the solution which leads to lower change of switching angles (α) from the previous m_d, is considered for storing in the processor memory. This leads to less no. of sections for the processor when a piecewise mixed model is considered for storing the entire switching angle curve. This technique is well suited for limiting voltage THD in two level grid connected VSI with L-C filter. The verification of theoretical concept is done in laboratory prototype of PV (500 W) connected to grid-tied PWM inverter. The control environment is realized in embedded FPGA interfaced national instrument hardware.**

***Index Terms*-- Selective Harmonics Elimination (SHE), Pulse Width Modulated (PWM) Inverter.**

I. Introduction

In last decade application of renewable energy sources such as PV and wind has escalated in power industry to combat climate change. But these sources are highly intermittent in nature and creates a challenge for continuous power supply [1]. Inverters are used for grid integration for solar PV system. Grid-tied inverters can be either current source inverter (CSI) or voltage source inverter (VSI) type [2]. Effectiveness in MPPT of series connected PV string can be enhanced by using CSI [3]. But this approach is having a major limitation of increased conduction loss in semiconductor switches compared to VSI for similar rating [4]. Again, ability of CSI with strict grid code such as fault ride through is questionable. In the last decade use of VSI like two level and multilevel for grid interfacing had investigated intensively [5]. Multilevel inverters have problem of inability to counter partial shading and it requires a large number of series connected PV cell to maintain DC link voltage. Cascaded multilevel inverter is better alternative but it reduces life of PV cell as it exposes low frequency ac component [6-8]. Real time selective harmonics elimination scheme is tested with PV tied multilevel inverter as proposed by F. Filho et.al [9]. But it has deficiency of increased complexity with feedback control. On the counterpart, two level inverters are still reliable for grid connected PV systems. However, they have limitations like switching losses and relatively low-quality output voltage [10]. To meet the strict grid code like IEEE 1574, IEC61727 [11] while interfacing medium voltage grid connected inverter, different advanced modulation strategies are used. Carrier based sinusoidal PWM or space vector PWM is mostly used for inverter control. Sinusoidal PWM is incapable of utilizing full DC link voltage, thus power density is less [12]. Compared to sinusoidal PWM, space vector PWM enhances use of semiconductor and DC link voltage. It increases switching frequency and has limitation of stable operation under unbalance operation in AC side [13]-[16]. Thus, finding a proper modulation strategy is challenging to meet strict grid code [16] with individual harmonics as a percentage of fundamental [11]. There are different topologies of filter presented in recent literatures for grid connected inverter where L-C, L-C-L filter are popular to support these grid code restrictions [17-18].

Different control topologies of inverter are researched to work with L-C-L filter while connected to grid. The main problem of L-C filter connected to inverter, is higher voltage THD compared to L-C-L filter of same size [19]-[24]. These mentioned issues of PWM techniques, grid codes and standard requirements can be eliminated by using traditional SHE based PWM [24-25]. The major issue of the SHE PWM techniques are that the solution of the transcendental equations requires numerical techniques to be solved. The online application becomes difficult due to increased computational burden in processor.

In the proposed work an improved selective harmonics elimination technique for PV assisted single phase grid-tied PWM inverter is implemented. Piecewise mixed linear model for storing switching angles for different modulation indexes (m_d) is adopted in proposed control. This technique is simple in implementation and provide low voltage THD at less filter size.

II. PV Assisted Grid-Tied Inverter System Modelling

Single phase grid tied PV model comprises of 500W solar PV, 100 Ah lead acid battery, buck-boost converter and inverter system. These components are modelled using dynamic equations in PSIM 9.1.1 simulation environment.

A. PV Modelling:

For simplicity in the analysis of single diode model of PV cell is considered [1] as shown in Fig.1.Thus, the output current from PV is

$I=I_{ph}-I_d-I_{sh}$ where

$$I_d=I_{se}\left[\exp\left(\frac{V+IR_{se}}{nV_t}\right)-1\right],\ I_{sh}=\frac{V+IR_{se}}{R_{sh}}.$$

Thus, $$I=I_{ph}-I_{se}\left[\exp\left(\frac{V+IR_{se}}{nV_t}\right)-1\right]-\frac{V+IR_{se}}{R_{sh}}$$ and $$V_t=\frac{T_cK}{q}$$

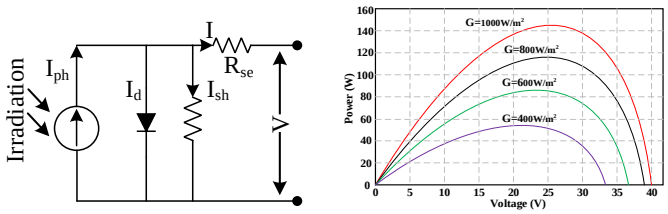

(a) (b)

Fig. 1 (a) Equivalent circuit model of PV cell (b) Output Characteristics of PV Cell.

B. Buck-Boost Converter:

Buck-boost converter is PV interfaced converter responsible to fix steady output voltage before inverter. The modelling equations [1] are,

$$\frac{d}{dt}\begin{bmatrix} i_L \\ v_C \end{bmatrix} = \begin{bmatrix} \frac{R_c(1+D)-R_L}{L_E} & \frac{(D-1)}{L_E} \\ \frac{(D-1)}{C} & \frac{(2D-1)}{RC} \end{bmatrix}\begin{bmatrix} i_L \\ v_C \end{bmatrix} + \begin{bmatrix} \frac{D}{L_E} \\ 0 \end{bmatrix} V_g \quad (2)$$

$$v_o = -\begin{bmatrix} (1-D)R_c & 1 \end{bmatrix}\begin{bmatrix} \frac{D}{L_E} \\ 0 \end{bmatrix} V_g$$

C. Voltage Source Inverter Modelling (VSI):

Linear inverter control with SHEPWM is applied for grid integration. Therefore, d-q model [26] is adopted in this work as shown in Fig. 2. The dynamic equations are,

$$\left.\begin{aligned} \frac{d}{dt}\begin{bmatrix} I_\alpha \\ I_\beta \end{bmatrix} &= \begin{bmatrix} u_\alpha \\ u_\beta \end{bmatrix}\frac{1}{L} - \begin{bmatrix} I_\alpha \\ I_\beta \end{bmatrix}\frac{1}{L}\left(r_L + \frac{Zr_c}{Z+r_c}\right) - \begin{bmatrix} V_\alpha \\ V_\beta \end{bmatrix}\left(\frac{1}{L} - \frac{r_c}{L(Z+r_c)}\right) \\ \frac{d}{dt}\begin{bmatrix} v_{\alpha c} \\ v_{\beta c} \end{bmatrix} &= \begin{bmatrix} I_\alpha \\ I_\beta \end{bmatrix}\frac{Z}{C(Z+r_c)} - \begin{bmatrix} V_\alpha \\ V_\beta \end{bmatrix}\frac{1}{C(Z+r_c)} \end{aligned}\right\} \quad (3)$$

Transformation matrix helps to find d-q model of single phase VSI from equation (3).

$$\begin{bmatrix} X_d \\ X_q \end{bmatrix} = T\begin{bmatrix} X_\alpha \\ X_\beta \end{bmatrix} \text{ where, } T = \begin{bmatrix} \cos\omega t & \sin\omega t \\ -\sin\omega t & \cos\omega t \end{bmatrix}$$

As parasitic elements are very small thus these are neglected in d-q modelling of VSI.

$$\left.\begin{aligned} \frac{d}{dt}\begin{bmatrix} I_d \\ I_q \end{bmatrix} &= \begin{bmatrix} u_d \\ u_q \end{bmatrix}\frac{1}{L} + \begin{bmatrix} 0 & -\omega \\ \omega & 0 \end{bmatrix}\begin{bmatrix} I_d \\ I_q \end{bmatrix} - \frac{1}{L}\begin{bmatrix} V_d \\ V_q \end{bmatrix} \\ \frac{d}{dt}\begin{bmatrix} v_d \\ v_q \end{bmatrix} &= \begin{bmatrix} I_d \\ I_q \end{bmatrix}\frac{1}{C} + \begin{bmatrix} 0 & -\omega \\ \omega & 0 \end{bmatrix}\begin{bmatrix} V_d \\ V_q \end{bmatrix} - \frac{1}{CZ}\begin{bmatrix} V_d \\ V_q \end{bmatrix} \end{aligned}\right\} \quad (4)$$

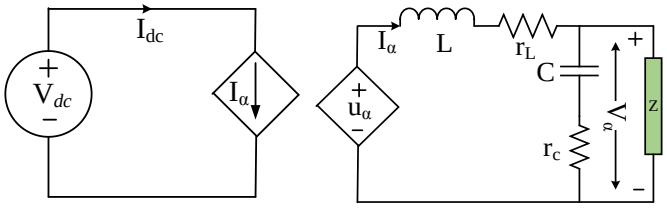

Fig. 2. Circuit model of single-phase inverter.

D. Lead Acid Battery Model with Current tracking:

The total system arrangement is shown in Fig. 6. Battery management is necessary due to intermittency of PV power. CIEMAT based dynamic battery model [27] is adopted in this work as shown in Fig. 3. Since the novelty of the work is not on battery management, on SOC information is not discussed in details.

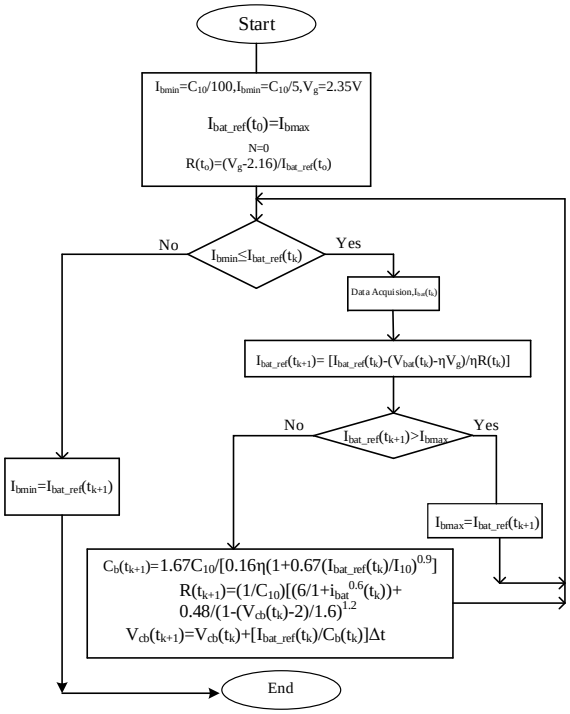

Fig. 3. CIEMAT Model based current tracking algorithm.

III. PROPOSED ALGORITHM OF SELECTIVE HARMONICS ELIMINATION TECHNIQUE

The proposed SHE technique is and its effectiveness on implementation is discussed below.

A. Harmonics Elimination in Bridge Inverter:

A generalized method to eliminate any number of harmonics is done by switching the voltage waveform. For a periodic inverter voltage waveform with unit amplitude this relationship is easily derived without losing generality. The voltage waveform for M number of switching per quarter cycle is shown in Fig. 4.

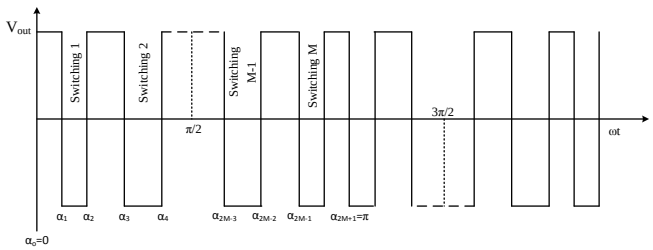

Fig. 4. Generalized SHE PWM voltage output of Inverter.

The waveform has property of half wave symmetry and fourier series of the waveform is,

$$f(\omega t)=\sum_{1,2,3}^{\infty}[b_n\sin(n\omega t)+a_n\cos(n\omega t)] \quad (6)$$

From Fig.3 $\alpha_0=0$, $\alpha_{2M+1}=\pi$ and $\alpha_0<\alpha_1<\alpha_2<\ldots<\alpha_{2M+1}$.the values of a_n and b_n is easily derived utilizing half wave symmetry property. For all odd values of n,

$$a_n=\frac{4}{n\pi}\left[-\sum_{k=1}^{2M}(-1)^k\sin(n\alpha_k)\right] \text{and,}$$

$$b_n=\frac{4}{n\pi}\left[1+\sum_{k=1}^{2M}(-1)^k\cos(n\alpha_k)\right]$$

The equation of a_n and b_n are functions of 2M variables (α_1, α_2, α_3, α_4,……, α_{2M}).In order to obtain an unique solution for the 2M variables , 2M equations are required. By equating M harmonics to zero value 2M equations are derived from a_n and b_n equations.

Again, applying quarter wave symmetry in Fig. 4 it is obvious that

$\alpha_k=\pi-\alpha_{2M-k+1}$ for k=1,2, 3, M and $a_n=0$.

Thus,

$$b_n=\frac{4}{n\pi}\left[1+2\sum_{k=1}^{M}(-1)^k\cos(n\alpha_k)\right] \quad (7)$$

M harmonics can be eliminated by solving M equation obtained from Eq.7. Newton-Raphson based linearized model is adopted to solve this equation to get switching angles for a modulation index.

The Eq. 7 can be generalized as

$f_i(\alpha_1,\alpha_2,\alpha_3,....,\alpha_M)=0$; for i=1,2, 3…. M.

Initially $\alpha^0=[\alpha_1^0,\alpha_2^0,.....,\alpha_M^0]^T$ can be calculated with guess value within 0 to π/2. Second step is to calculate $f(\alpha^0)=f^0$.

Linearizing the Eq. 7 about α^0

$$f^0+\left[\frac{df}{d\alpha}\right]^0=0$$

where, $\left[\frac{df}{d\alpha}\right]^0=\begin{bmatrix}\frac{df_1}{d\alpha_1} & . & \frac{df_1}{d\alpha_M}\\ . & . & .\\ \frac{df_M}{d\alpha_1} & . & \frac{df_M}{d\alpha_M}\end{bmatrix}$

Evaluating at α^0 and $d\alpha=[d\alpha_1,d\alpha_2,d\alpha_3,\ldots.d\alpha_M]^T$ solution of linearized Eq.7 is found. This process is again repeated to determine accurate switching angles ($\alpha^1=\alpha^0+d\alpha$). The degree of accuracy is determined for small value of error ε.

It is necessary condition to satisfy the final switching angles to follow $0<\alpha_1<\alpha_2<....<\alpha_M<\frac{\pi}{2}$.

$$\left[\frac{df}{d\alpha}\right]=\begin{bmatrix}2n_1\sinn_1\alpha_1 & -2n_1\sinn_1\alpha_2/. & \pm2n_1\sinn_1\alpha_M\\ \frac{2n_2\sinn_2\alpha_1}{.} & -2n_2\sinn_2\alpha_2/. & \frac{\pm2n_2\sinn_2\alpha_M}{.}\\ 2n_M\sinn_M\alpha_1 & -2n_M\sinn_M\alpha_2/. & \pm2n_M\sinn_M\alpha_M\end{bmatrix}$$

In order to solve matrix of Eq.7 must be non-singular. This condition is violated is anyone α_1, α_2, α_3, α_4,……, α_M is equal to zero when the domain of solution is within the interval [0.π/2]. Also, is any two α are equal, two columns of the matrix shall be identical, except for the sign, which may be opposite. The rank of the matrix in that case reduced to M-1, and the matrix will be singular.

Thus, the condition $0<\alpha_1<\alpha_2<....<\alpha_M<\frac{\pi}{2}$ ensures the non-singularity of matrix and a meaningful solution of Eq.7.

In the proposed algorithm as shown in Fig. 5, when the solution of a particular modulation index (m_d) leads to a drastic change of α from previous m_d, a repetitive set of initial guesses is tried to achieve α nearer to previous value of m_d. In the proposed algorithm 100 times repetition of initial value of α is taken. This is required to reduce the number of sections to store variation of α with m_d which ensures reduced memory burden of the processor. In some case there is no solution for a particular m_d and then discontinuation of α leads to unsuccessful while implemented for online application.

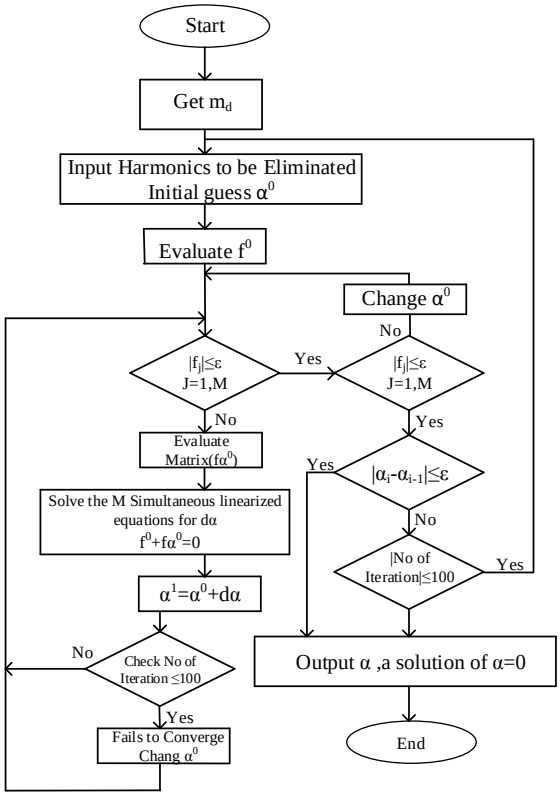

Fig. 5 Flowchart of proposed SHE Technique.

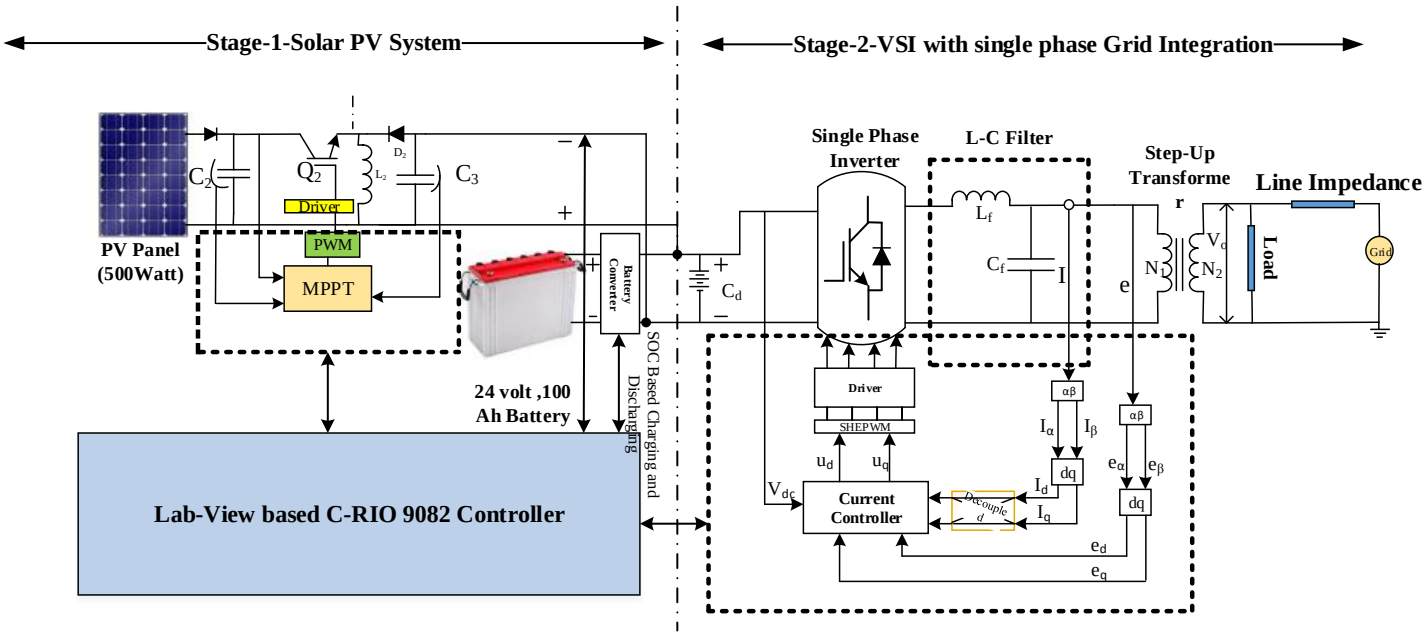

Fig. 6. Proposed System Arrangement.

In the proposed technique the amplitude of higher order harmonics is maintained at lower value while eliminating lower order harmonics. This technique ensures a continuous α value with modulation index (m_d) variation. Again, it also lowers the switching frequency helping to maintain THD at lower value and suitable for online closed loop system application.

B. The Effectiveness of the Proposed SHE Technique:

The proposed technique is superior over other SHE techniques in literature as it has several advantages like (a) linear change in modulation index (md). (b) Increase in modulation index (md) range (c) Piecewise mixed model suitable for closed loop operation.

(a) Linear change in modulation index (m_d)

Sometimes solutions of equation 7 leads to discontinuation of α for a particular modulation index. Thus, it creates complexity in practical implementation.

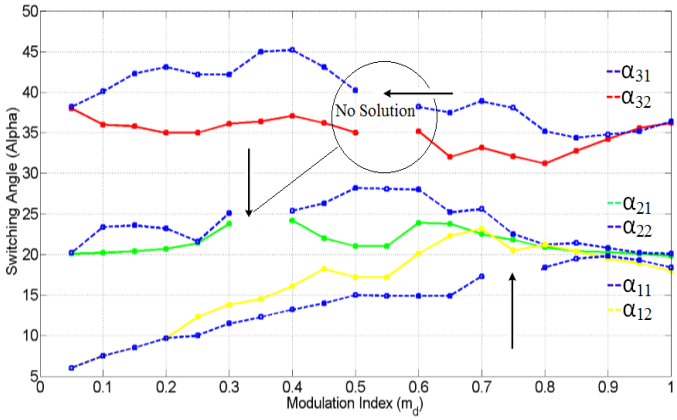

(a)

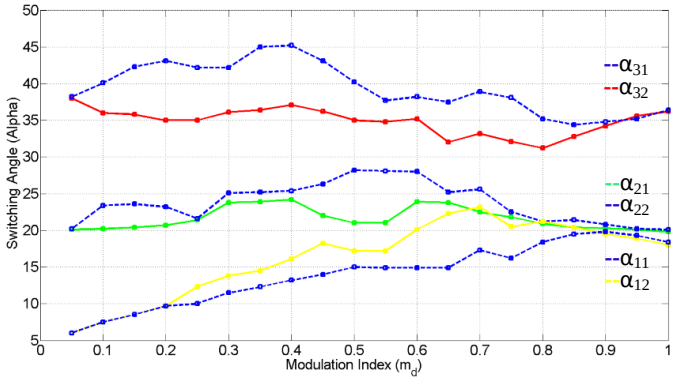

(b)

Fig. 7 (a) Discontinuous switching angle with modulation index variation [conventional] (b) Continuous switching angle with modulation index variation [proposed]

The amplitude of higher order harmonics is considered as a small value instead of zero. The difficulty shown in Fig 7 (a), where the 5th, 7th and 11th harmonic were set to zero is overcome by equating the same order of harmonics to 5th and 7th to zero and 11th to 1%. The solution is achieved for all the angles at all modulation indices (m_d). The revised plot is shown in Fig.7 (b). Here, α_{11} and α_{12} are the two values of α_1. Similarly, α_{21}, α_{22} and α_{31}, α_{32} are for α_2 and α_3 respectively. This also eliminates the possibility of divergence in finding solutions.

(b) Increment in modulation index range

SHE technique tends to produce switching angles in narrow range closed to zero especially when m_d>1. The proposed technique produces linear variation in switching angle above modulation index 1 as shown in Fig. 8. Typically, up to m_d=1.16 operation is possible with the proposed SHE technique.

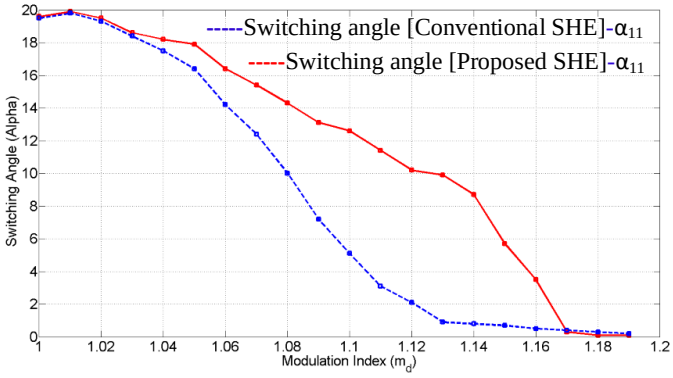

Fig. 8 switching angle with modulation index (m_d) variation [conventional-blue line] and switching angle with modulation index (m_d) variation [Proposed-Red line].

(c) Piecewise mixed model suitable for closed loop operation

SHE PWM requires larger memory space to store the switching angles for different modulation index (m_d). Again, it has inability to produce exact switching angles under dynamic operating condition under different modulation index (m_d). Thus, to reduce burden in microcontroller memory usage and to produce uniform modulation index under dynamic operation piecewise mixed model [28] is used. The well-known least squares curve-fitting technique [29]is applied to the curve to obtain coefficients a, b, and c. Then, the number of points n considered is increased, and the sum-squared error F (e^2) given as follows is computed until the error for that portion is within the specified limit, which is 10^{-1} in this case.

$$F\left(e^2\right)=\sum_{k=1}^{n}(\alpha_k-(am_d^2+bm_d+c))^2$$

For the section where the curve is linear, the constant "a" shall be zero or less than some minimum specified value, which is 10^{-3} here. Thus, the required minimum numbers of linear and nonlinear equations are formed to represent the switching angle variation curve. From the switching angle variation curve as shown in Fig. 9, the "piecewise mixed model" equations are derived.

$\alpha_{11}=24.66m_d$; for $0.05\le m_d\le 0.5$,

$\alpha_{11}=3m_d+13.5$ for $0.5\le m_d\le 0.75$, $\alpha_{11}=0.67m_d^2+6.7m_d+11.4$ for $0.75\le m_d\le 0.9$ and $\alpha_{11}=-0.3m_d+21.5$.

Only four set of equation is required to calculate switching angle for α_{11} under different modulation index (m_d) ranges from 0.05 to 1.

Table-I
Computational Burden [Software and hardware]

Software				Hardware	
For 3rd and 5th harmonics	Error	Computational Time	Divergence Protection	RAM Usage (MB)	Overflow for M>1
Conventional SHEPWM	3.2×10^{-5}	2.01 sec.	No	0.26	Yes
Proposed SHEPWM	4.1×10^{-5}	1.80862 sec.	Yes	0.18	No

Thus, using these piecewise mixed equations memory burden to microprocessor is reduced. Comparison of computational burden between proposed SHEPWM and conventional SHEPWM is given in Table-I.

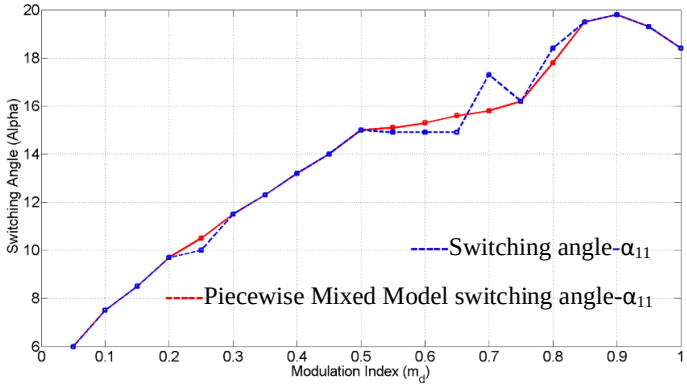

Fig. 9 switching angle with modulation index (m_d) variation [conventional-blue line] and switching angle with modulation index (m_d) variation [Proposed SHE with Mixed Model-Red line].

IV. SIMULATION AND EXPERIMENTAL RESULT

Simulation in PSIM 9.1.1 and hardware study is done to verify effectiveness of proposed SHE on single phase grid tied PV system as shown in Figs.6 and 10.

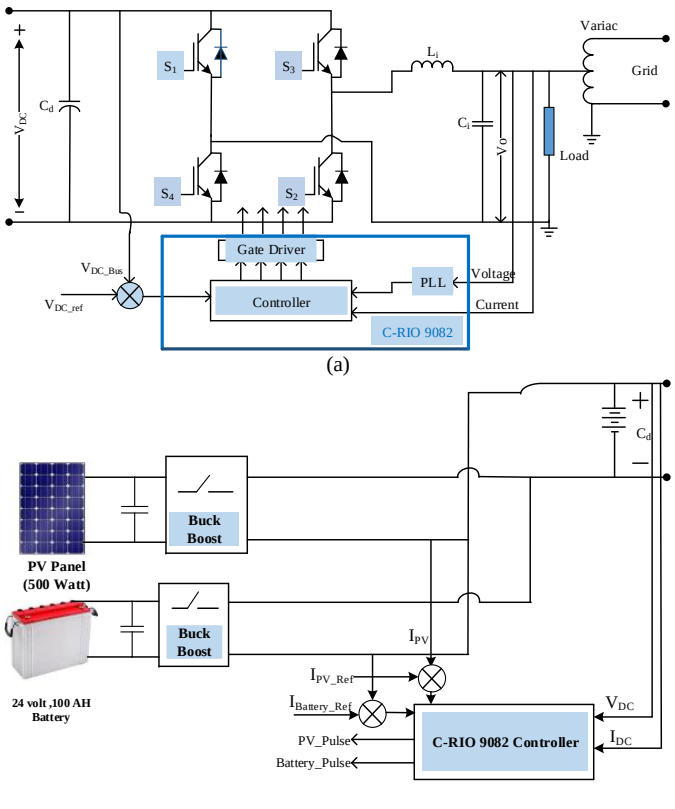

Fig. 10. (a) Inverter control Section. (b) PV tied converter control with battery.

Proposed SHEPWM based control scheme with L-C filter guarantees low voltage THD. This is shown in Fig.11 and Table-II.

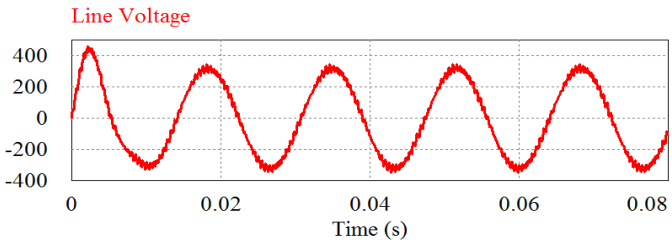

Fig. 11. Line voltage after L-C filter.

Table-II
Percentage (%) of Fundamental Voltage Harmonics @Simulation Result

Harmonics	1	3	5	7	9	11	13	15	17
	100	0.1	0.3	0.2	0.09	0.15	0.15	0.01	0.01

Fig. 12 (a) shows the experimental switching waveform for eliminating 5th and 7th harmonics. The harmonics elimination is obtained by programming in Lab-view c-RIO 9082 on 9401 module, and the switching angles are 16.247°, 22.068° respectively.

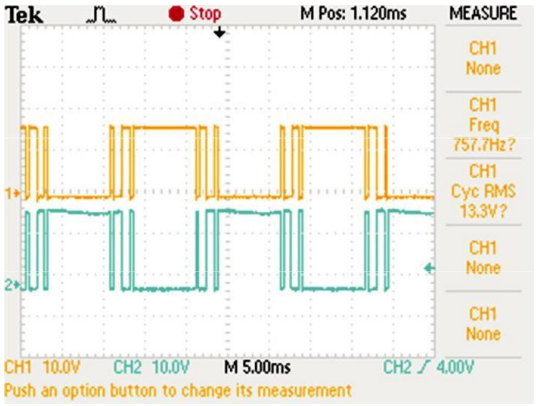

(a)

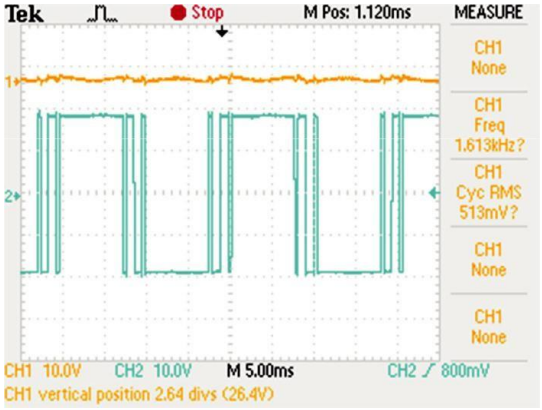

(b)

Fig. 12. (a) Switching waveform for eliminating 5th and 7th harmonics (b) Inverter output waveform for eliminating 5th and 7th harmonics.

The corresponding inverter output voltage is shown in Fig. 12 (b). Similarly the switching angles for eliminating 5th , 7th ,11th , and maintaining 13th harmonics within lower value as discussed in section III are found as 10.545°,16.092°, 30.904° and 32.866° respectively as shown in Fig. 13 (a). The inverter output voltage is shown is Fig. 13 (b).

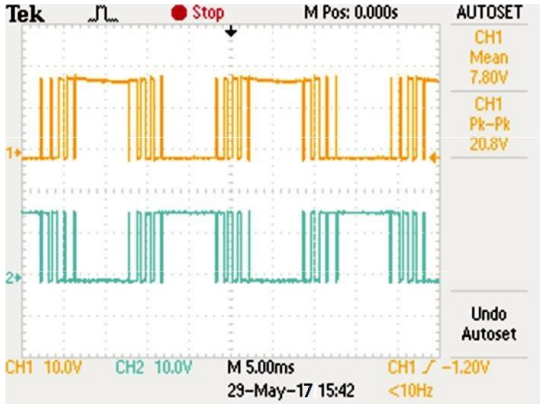

(a)

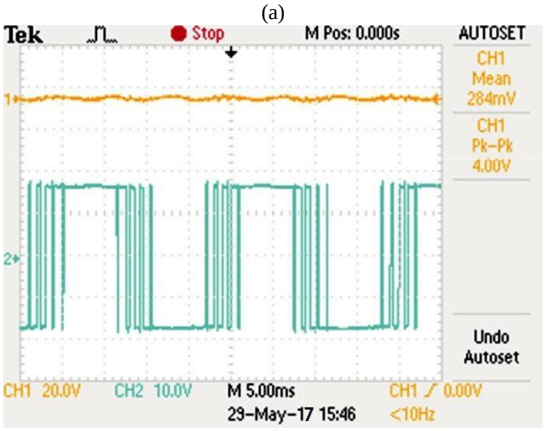

(b)

Fig. 13. (a) Switching waveform for eliminating 5th, 7th, 11th and 13th harmonics (b) Inverter output waveform for eliminating 5th, 7th, 11th and 13th harmonics.

The inverter output voltage using SHE PWM is shown in Fig.18 (a). The FFT of the output voltage is shown in Fig. 14 (c). The Voltage THD value is 5.7 % and measured in power quality analyzer Aplab PQA2100E and individual harmonics contents are listed in Table IV.

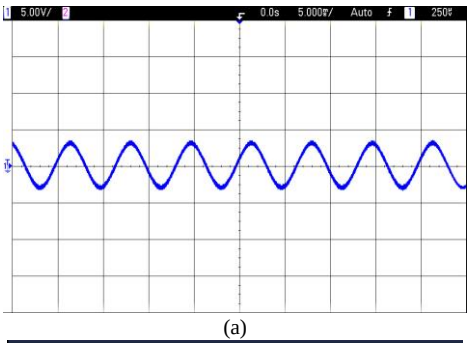

(a)

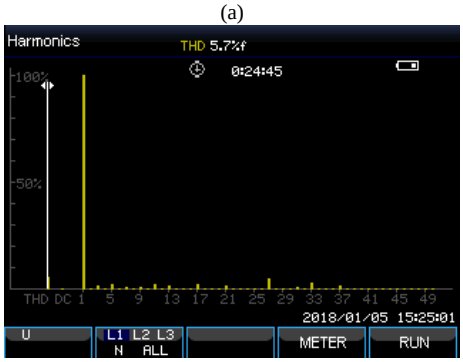

(b)

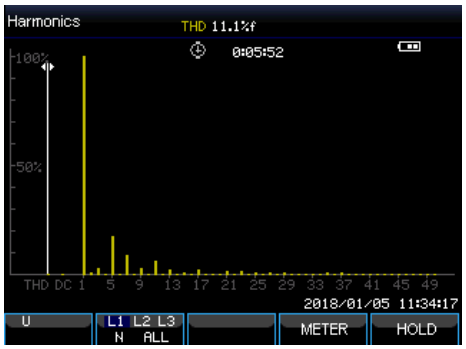

(c)

Fig. 14. (a) Voltage output after L-C filter (Transformer input). (b) FFT of voltage using conventional PI control of inverter. (c) FFT of voltage using proposed SHE PWM control.

It is found that the with same filter size THD value with conventional control of inverter is higher i.e. 11.1 % as shown in Fig. 14 (b). The comparative study shown in Table-III shows the effectiveness of the proposed control and it is found better than L-C-L type filter-based control with less complexity.

Table-III
Comparative Table between Different Controllers

PI Control with L-C Filter	SHE PWM with L-C Filter	Control with L-C-L Filter [18-19]
L:90uH., C:3uH Voltage THD: 11.1%	L:90uH., C:3uH Voltage THD:5.7%	L_1:5.5mH, L2:1mH, C: 20uF. Voltage THD:5.067%

It is clear from Table-III that SHEPWM based linear control with L-C filter gives comparable voltage THD result with proportional resonant (PR) controller-based L-C-L filter system. Classical PI control with sinusoidal PWM inverter control with L-C filter has voltage THD is about 11.1% which is around 5% and 6% more than other methods. Thus, the proposed SHEPWM based control is capable of replacing complex PR control scheme with LCL filter. Though proposed method has 0.633% more voltage THD, it can be further improved by increasing capacitor value from 3uF to (5-10) uf. The proposed control scheme is modelled and implemented in 2-kHz switching frequency. The L-C filter size can be further minimized by increasing switching frequency. But this comes with complexity in determining firing angle for eliminating 3rd and 5th harmonics with different modulation index.

Table-IV
Percentage (%) of Fundamental Voltage Harmonics @ Proposed SHE PWM Experimental Result

Harmonics	1	3	5	7	9	13	17	27	33
	100	0.05	0.2	0.1	0.1	0.3	0.15	0.25	0.20

Total control of source side PV, battery and inverter as shown in Fig. 15 is done in Lab view c-RIO 9082 using system parameter in Table V.

Table-V
Parameters for Prototype System

Inverter (VA)	PV Panel	Battery	Active Power	Reactive Power	F_{SW} kHz	F_{Grid} Hz	Tr Ratio
1200	500W	100Ah	500W	300Var	2	50	1:10

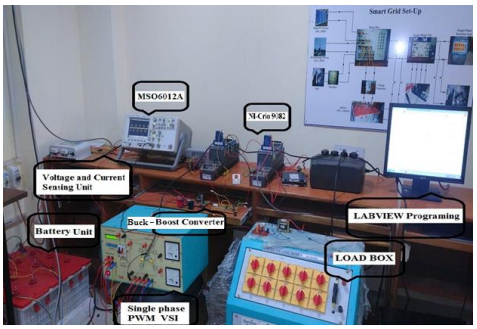

(a)

(b)

Fig. 15. (a) Single phase grid tied VSI with lead acid battery. (b) 500-Watt PV panel.

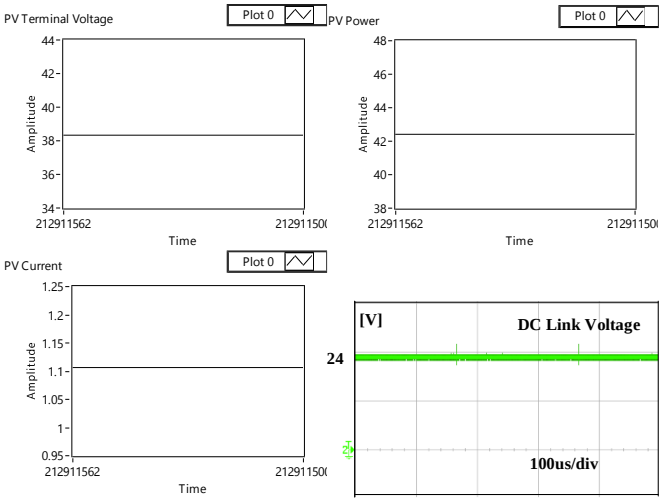

Fig. 16. (i) PV side voltage, power and current monitoring using waveform chart in Lab-View front panel. (ii) Different control variable in PV converter side control.

Fig. 16 shows the online PV voltage, PV power and common DC link stable voltage. The dynamic pulse of MPPT is shown in Fig. 16 (ii) (c).

During load change DC link voltage, and current changes stably as shown in Fig. 17. (a).and (c) respectively.

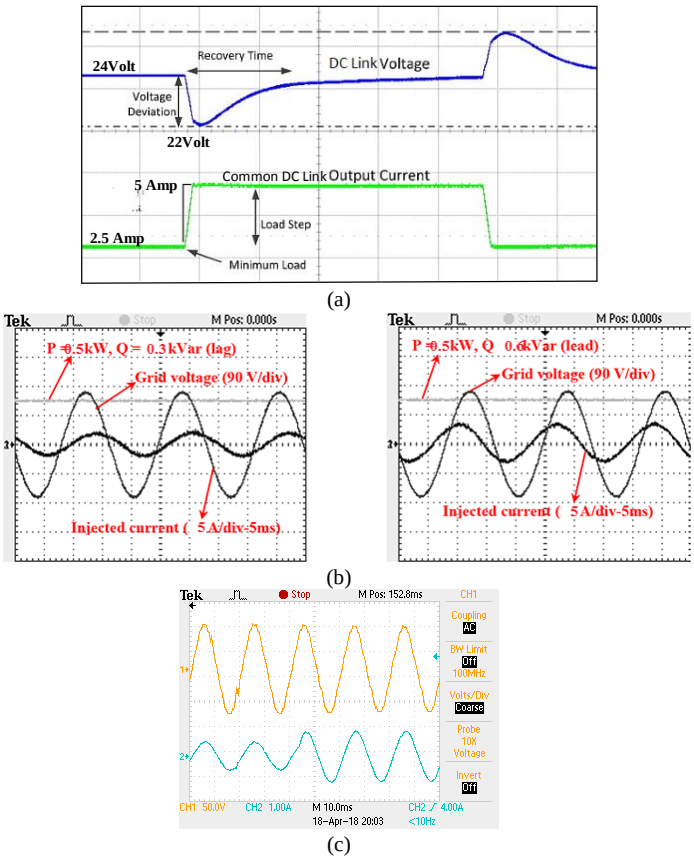

Fig. 17 (a) DC bus voltage for step load change. (b) Grid tied Active power and reactive power. (c) Stable Line voltage and line current after L-C filter during load change [Resistive].

V. CONCLUSION

In the presented work an improved selective harmonics elimination technique for PV assisted single phase grid-tied PWM inverter is implemented. This technique gives best result in voltage THD (5.7%) with low value L-C filter compared to conventional PI based control of same filter size (11.1%). It is effective as control scheme is simple unlike L-C-L based filter system and low voltage THD value while connected to single phase grid. The proposed technique is tested in 500W single phase grid tied solar PV system.

The achievements of applying the proposed techniques are

(a) Low voltage THD is achieved using proposed piecewise linear model of SHEPWM suitable for online application.

(b) L-C filter size is comparable to PR controlled LCL filter system.

(c) Easy control scheme and low-cost microcontroller (TMS320F28379D) can easily be used for single phase PV tied grid connected system.

(d) Flexibility in mitigating individual harmonics content using less burden on processor.

REFERENCES

[1] C. S. Solanki, "Solar Photovoltaics Fundamentals, Technologies and Applications", 2nd Edition New Delhi, India: PHI Learning Private Limited, 2011.

[2] S. B. Kjaer, J. K. Pedersen, and F. Blaabjerg, "A review of single-phase grid-connected inverters for photovoltaic modules," *IEEE Transactions on Industrial Application*., vol. 41, no. 5, pp. 1292–1306, Sep.–Oct. 2005

[3] R. Gonzalez, J. Lopez, P. Sanchis, and L. Marroyo, "Transformerless inverter for single-phase photovoltaic systems," *IEEE Transactions on Power Electronics*, vol. 22, no. 2, pp. 693–697, Mar. 2007.

[4] H. Hu, S. Harb, D. Zhang, X. Fang, Q. Zhang, J. Shen, and I. Batarseh,"A three-port flyback for PV microinverter applications with power pulsation decoupling capability," *IEEE Transactions on Power Electronics*, vol. 27, no. 9, pp. 3953–3964, Sep. 2012.

[5] S. Alepuz, S. Busquets-Monge, J. Bordonau, J. Gago, D. Gonzalez, and J. Balcells, "Interfacing renewable energy sources to the utility grid using a three-level inverter," *IEEE Transactions on Industrial Electronics*, vol. 53, no. 5, pp. 1504–1511, Oct. 2006.

[6] Nasser Ahmed Al-Emadi, Concettina Buccella, Carlo Cecati, Hassan Abdullah Khalid, "A novel DSTATCOM with 5-level CHB architecture and selective harmonic mitigation algorithm", *Electric Power Systems Research*, Vol. 130, pp. 251-258, Jan. 2016.

[7] Mohamed S.A. Dahidah, Vassilios G. Agelidis, "Single-carrier sinusoidal PWM-equivalent selective harmonic elimination for a five-level voltage source converter", *Electric Power Systems Research*, Vol 78, Issue 11,pp.1826-1837, Nov. 2008.

[8] Bakhshizadeh, Mohammad Kazem, Hossein Iman-Eini, and Frede Blaabjerg. "Selective harmonic elimination in asymmetric cascaded multilevel inverters using a new low-frequency strategy for photovoltaic applications." *Electric Power Components and Systems* vol.43, no.8, pp. 964-969, Oct 2015.

[9] F. Filho, L. M. Tolbert, Y. Cao and B. Ozpineci, "Real-Time Selective Harmonic Minimization for Multilevel Inverters Connected to Solar Panels Using Artificial Neural Network Angle Generation," in *IEEE Transactions on Industry Applications*, vol. 47, no. 5, pp. 2117-2124, Sept.-Oct. 2011.

[10] Y. Bo, L.Wuhua, Z. Yi, and H. Xiangning, "Design and analysis of a grid connected photovoltaic power system," *IEEE Transactions on Power Electronics*, vol. 25, no. 4, pp. 992–1000, Apr. 2010.

[11] IEEE Standard for Interconnecting Distributed Resources With Electric Power Systems," *IEEE Standard* 1547, 2003

[12] Z. Keliang and W. Danwei, "Relationship between space-vector modulation and three-phase carrier-based PWM: A comprehensive analysis [three-phase inverters]," *IEEE Transactions on Industrial Electronics*, vol. 49, no. 1, pp. 186–196, Feb. 2002.

[13] G. Konstantinou, V.G. Agelidis, On re-examining symmetry of two-level selective harmonic elimination PWM: Novel formulations, solutions and performance evaluation, *Electric Power Systems Research*, Vol. 108, pp. 185-197, Mar. 2014.

[14] V. G. Agelidis, A. I. Balouktsis, andM. S. A. Dahidah, "A five-level symmetrically defined selective harmonic elimination PWMstrategy: Analysis and experimental validation," *IEEE Transactions on Power Electronics*, vol. 23, no. 1, pp. 19–26, Jan. 2008.

[15] V. G. Agelidis, A. Balouktsis, I. Balouktsis, and C. Cossar, "Multiple sets of solutions for harmonic elimination PWM bipolar waveforms: Analysis and experimental verification,"

IEEE Transactions on Power Electronics, vol. 21, no. 2, pp. 415–421, Mar. 2006.

[16] K.Yang, Z.Yuan,R.Yuan,W.Yu,J.Yuan and J.Wang, " A Groebner based Theory-Based Method for Selective Harmonics Elimination," *IEEE Transactions on Power Electronics*, vol.30, no.12,pp.6581-6592,Dec.2015.

[17] F. Liu, Y. Zhou, S. Duan, J. Yin, B. Liu and F. Liu, "Parameter Design of a Two-Current-Loop Controller Used in a Grid-Connected Inverter System With LCL Filter," in *IEEE Transactions on Industrial Electronics*, vol. 56, no. 11, pp. 4483-4491, Nov. 2009.

[18] K. H. Ahmed, S. J. Finney and B. W. Williams, "Passive Filter Design for Three-Phase Inverter Interfacing in Distributed Generation," *2007 Compatibility in Power Electronics*, Gdansk, 2007, pp. 1-9.

[19] S. Kouro, J. I. Leon, D. Vinnikov and L. G. Franquelo, "Grid-Connected Photovoltaic Systems: An Overview of Recent Research and Emerging PV Converter Technology," in *IEEE Industrial Electronics Magazine*, vol. 9, no. 1, pp. 47-61, March 2015.

[20] G. Shen, X. Zhu, J. Zhang and D. Xu, "A New Feedback Method for PR Current Control of LCL-Filter-Based Grid-Connected Inverter," in *IEEE Transactions on Industrial Electronics*, vol. 57, no. 6, pp. 2033-2041, June 2010.

[21] M. Prodanovic and T. C. Green, "Control and filter design of three-phase inverters for high power quality grid connection," in *IEEE Transactions on Power Electronics*, vol. 18, no. 1, pp. 373-380, Jan 2003.

[22] J. C. Giacomini, L. Michels, H. Pinheiro and C. Rech, "Design methodology of a passive damped modified LCL filter for leakage current reduction in grid-connected transformerless three-phase PV inverters," in *IET Renewable Power Generation*, vol. 11, no. 14, pp. 1769-1777, 12 13 2017.

[23] J. Xu, S. Xie, L. Huang and L. Ji, "Design of LCL-filter considering the control impact for grid-connected inverter with one current feedback only," in *IET Power Electronics*, vol. 10, no. 11, pp. 1324-1332, 9 9 2017.

[24] T. F. Wu, M. Misra, L. C. Lin and C. W. Hsu, "An Improved Resonant Frequency Based Systematic LCL Filter Design Method for Grid-Connected Inverter," in *IEEE Transactions on Industrial Electronics*, vol. 64, no. 8, pp. 6412-6421, Aug. 2017.

[25] T. Kato, K. Inoue and M. Ueda, "Lyapunov-Based Digital Control of a Grid-Connected Inverter With an LCL Filter," in *IEEE Journal of Emerging and Selected Topics in Power Electronics*, vol. 2, no. 4, pp. 942-948, Dec. 2014.

[26] J.F.Sultani, "Modelling, Design and Implementation of D-Q Control in Single Phase Grid Connected Inverters for Photovoltaic Systems used in Domestic Dwellings", *PhD Thesis, De Montfort University, Leicester, UK, 2013*. URI: http://hdl.handla.net/2086/9631.

[27] J. B. Copetti and F. Chenlo, ''A general battery model for PV system simulation,'' J. Power Sources, vol. 47, pp. 109–118, 1994.

[28] D. Chatterjee, "A Novel Magnetizing-Curve Identification and Computer Storage Technique for Induction Machines Suitable for Online Application," in *IEEE Transactions on Industrial Electronics*, vol. 58, no. 12, pp. 5336-5343, Dec. 2011.

[29] Geer Sara A. "Least Square estimation", Wiley Journal, 15th October 2005. doi: 10.1002/0470013192.bsa199.